

Lewis Acid Trapping of an Elusive Copper–Tosylnitrene Intermediate Using Scandium Triflate

Subrata Kundu,[†] Enrico Miceli,[†] Erik Farquhar,[‡] Florian Felix Pfaff,[†] Uwe Kuhlmann,[§] Peter Hildebrandt,[§] Beatrice Braun,[†] Claudio Greco,[†] and Kallol Ray*,[†]

[†]Institut für Chemie, Humboldt-Universität zu Berlin, Brook-Taylor-Straße 2, D-12489 Berlin, Germany

[‡]Case Western Reserve University Center for Synchrotron Biosciences and Center for Proteomics and Bioinformatics, National Synchrotron Light Source, Brookhaven National Laboratory, Upton, New York 11973, United States

[§]Institut für Chemie, Technische Universität Berlin, Sekr. PC14, Straße des 17 Juni 135, D-10623 Berlin, Germany

Supporting Information

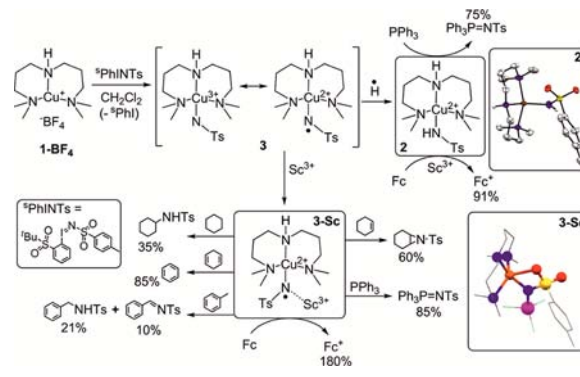
ABSTRACT: High-valent copper–nitrene intermediates have long been proposed to play a role in copper-catalyzed aziridination and amination reactions. However, such intermediates have eluded detection for decades, preventing the unambiguous assignments of mechanisms. Moreover, the electronic structure of the proposed copper–nitrene intermediates has also been controversially discussed in the literature. These mechanistic questions and controversy have provided tremendous motivation to probe the accessibility and reactivity of Cu^{III}–NR/Cu^{II}–N[•]R species. In this paper, we report a breakthrough in this field that was achieved by trapping a transient copper–tosylnitrene species, **3-Sc**, in the presence of scandium triflate. The sufficient stability of **3-Sc** at –90 °C enabled its characterization with optical, resonance Raman, NMR, and X-ray absorption near-edge spectroscopies, which helped to establish its electronic structure as Cu^{II}–N[•]Ts (Ts = tosyl group) and not Cu^{III}NTs. **3-Sc** can initiate tosylation of cyclohexane, thereby suggesting Cu^{II}–N[•]Ts cores as viable reactants in oxidation catalysis.

Terminal copper–nitrene units have been proposed as reactive intermediates in a number of copper-catalyzed alkane amination and alkene aziridination reactions.^{1–4} Understanding the structures, properties, and reactivities of such species is critical for obtaining mechanistic insights into oxidation catalysis and developing new, selective catalytic reagents and processes. Although examples of isolated nitrenes of late transition metals such as Fe,^{5a} Co,^{5b} and Ni^{5c} are known, direct spectroscopic characterizations of copper–nitrene intermediates have not been reported, leaving the mechanism ambiguous. Examples of such species have been characterized only through theoretical calculations.⁶ The nature of their ground state is also ambiguous. The singlet state (with a bent nitrene coordination mode) and the triplet state (with linear nitrene coordination) were theoretically calculated to be very close in energy, and the predicted ground state was found to depend strongly on the computational method used.⁶ We report herein the Lewis acid trapping of an elusive copper–tosylnitrene (Cu^{II}–N[•]Ts) species, **3-Sc**, in the presence of Sc(OTf)₃ in near-quantitative yields and

its detailed characterization by spectroscopy and theory, which enabled an unambiguous assignment of its electronic structure. Moreover, complex **3-Sc** comprising the Cu^{II}–N[•]Ts core rapidly abstracts H atoms from the strong C–H bonds of cyclohexane, thus providing a key precedent for the possible involvement of Cu^{II}–N[•]Ts in oxidation catalysis.

The reaction of the complex [Cu(L1)](BF₄) (**1-BF₄**) [L1 = 3,3'-iminobis(*N,N*-dimethylpropylamine)]⁷ with 2 equiv of [*N*-(*p*-toluenesulfonyl)imino](2-*tert*-butylsulfonyl)phenyliodinane (^sPhINTs)⁸ at 25 °C resulted in the immediate formation of the bluish-green complex **2** (Scheme 1). Greenish-blue crystals

Scheme 1. Formation and Reactivity of **2** and **3-Sc**^a



^aColor code: Sc, purple; N, blue; S, yellow; O, red; Cu, orange; C, gray.

suitable for X-ray diffraction [Table S1 in the Supporting Information (SI)] were obtained by layering of hexane onto a dichloromethane solution of **2**. The molecular structure of **2** determined by X-ray crystallography shows a four-coordinate copper–tosylamide complex cation (Scheme 1) with the geometry of copper being best described as distorted tetrahedral. The Cu–N_{amide} distance of 1.934(2) Å is comparable to that reported for other Cu^{II}–sulfonamide complexes [1.921(2)–1.954(7) Å].⁹ The absorption spectrum of **2** displays a broad, low-intensity band at λ_{max} [ε_{max}] = 660 nm [250 M⁻¹ cm⁻¹] and extending from 550 to 1050 nm, which is assigned to the low-

Received: July 9, 2012

Published: August 28, 2012

energy d–d transitions arising from an $S = 1/2$ d^9 Cu^{II} center in a pseudotetrahedral geometry (Figure 1 top; dash-dotted line).

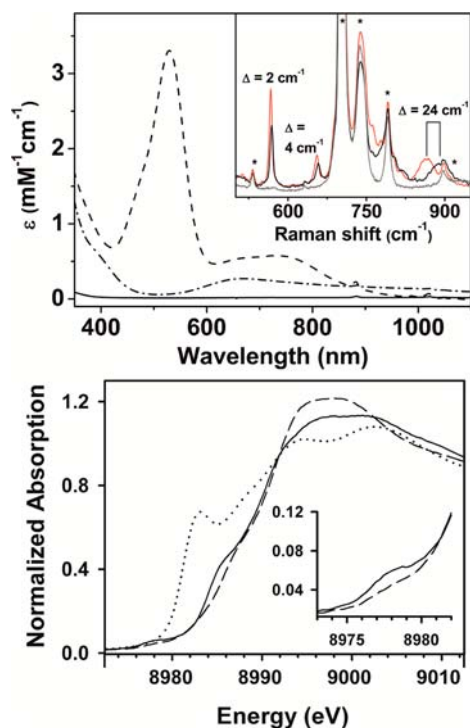


Figure 1. Top: Absorption spectra of **1-BF₄** (solid line), **2** (dash-dotted line), and **3-Sc** (dashed line) in CH_2Cl_2 at -90 °C. Inset: rR spectra of **3-Sc-¹⁴N** (black), **3-Sc-¹⁵N** (red) and the **3-Sc** decay product at room temperature (gray) upon excitation at 514 nm. Bands originating from the solvent are marked with asterisks. Bottom: Normalized XANES spectra of **1-BF₄** (dotted line), **2** (solid line), and **3-Sc** (dashed line). The inset depicts an expansion of the pre-edge region for **2** and **3-Sc**.

The X-band electron paramagnetic resonance (EPR) spectrum of the sample frozen to -263 °C after mixing of **1-BF₄** and $^5\text{PhINTs}$ at 25 °C (Figure S1 in the SI) shows a slightly rhombic signal with g values ($g_x = 2.09$, $g_y = 2.07$, $g_z = 2.27$) and hyperfine constants ($A_x = 54 \times 10^{-4} \text{ cm}^{-1}$, $A_y = 15 \times 10^{-4} \text{ cm}^{-1}$, $A_z = 128 \times 10^{-4} \text{ cm}^{-1}$) consistent with the $d_{x^2-y^2}$ ground state of the Cu^{II} center.¹⁰ Spin quantitation based on the EPR signal indicated that at least 95% of the centers contained EPR detectable monomeric Cu^{II} species.

The conversion of **1-BF₄** to **2** in the presence of $^5\text{PhINTs}$ presumably involves the initial formation of a transient Cu -nitrene intermediate, **3**, followed by rapid H-atom abstraction from the solvent and/or adventitious water (Scheme 1). We therefore sought to trap the elusive $\text{Cu}^{\text{III}}\text{-NTs}/\text{Cu}^{\text{II}}\text{-N}^{\bullet}\text{T}$ s intermediate **3** before its conversion to **2** and demonstrate its reactivity in a number of group transfer reactions. Monitoring of the reaction of **1-BF₄** with $^5\text{PhINTs}$ in CH_2Cl_2 by UV-vis spectroscopy over a range of temperatures from room temperature to -90 °C, however, did not lead to the accumulation or observation of any intermediate species competent for alkane or alkene substrate oxidation. A near-quantitative yield of the Cu^{II} species was obtained even at temperatures as low as -90 °C. We then tried to trap **3** in the presence of a Lewis acid, a strategy that we successfully used previously to stabilize an elusive $S = 3/2$ oxocobalt(IV) complex.¹¹ Indeed, a metastable intermediate with an intense purple color exhibiting absorption maxima centered at $\lambda_{\text{max}} [\epsilon_{\text{max}}] = 530 \text{ nm} [3500 \text{ M}^{-1} \text{ cm}^{-1}]$ and 750 nm

$[580 \text{ M}^{-1} \text{ cm}^{-1}]$ (Figure 1 top; dashed line) was obtained when 1 equiv of $\text{Sc}(\text{OTf})_3$ was used in the reaction.¹² Interestingly, the 530 nm absorption feature of the new intermediate resembles that reported by Tolman and co-workers¹³ for a $\text{Cu}^{\text{III}}\text{-OH}$ complex and by King et al.¹⁴ for the corresponding aryl- $\text{Cu}^{\text{III}}\text{-X}$ complexes ($X = \text{Cl}, \text{Br}, \text{I}$). Generation of the purple intermediate, designated as **3-Sc**, was found to be complete immediately upon addition of the oxidant $^5\text{PhINTs}$ to a CH_2Cl_2 solution of **1-BF₄** and $\text{Sc}(\text{OTf})_3$ at -90 °C, after which it slowly decayed to a Cu^{I} species¹⁵ with a half-life of 1600 s (Figure S2). In contrast to the doublet ($S = 1/2$) ground state of **2**, **3-Sc** is diamagnetic ($S = 0$), as demonstrated by the ^1H NMR resonances spread over a chemical shift range of 0 to +10 ppm (Figure S3).

3-Sc underwent a two-electron reduction process with a one-electron reductant such as ferrocene (Fc) at -90 °C with the corresponding formation of a Cu^{I} species¹⁵ and ferrocenium cations (Fc^+ ; 180% yield) (Figure 2); this confirmed that **3-Sc** is

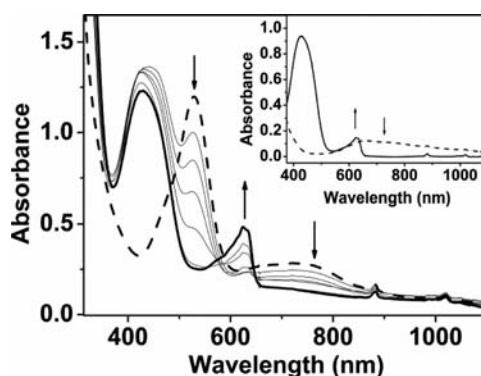


Figure 2. Changes in the absorption spectra associated with the reaction of **3-Sc** (0.34 mM) with ferrocene (30 equiv) at -90 °C. Inset: Absorption spectra of **2** (dashed line) (0.36 mM) and the product of its reaction with ferrocene (30 equiv) in the presence of 1 equiv of $\text{Sc}(\text{OTf})_3$ (solid line) at -90 °C. The yield of Fc^+ was determined on the basis of the known extinction coefficient of its 620 nm band in CH_2Cl_2 at -90 °C ($\epsilon = 505 \text{ M}^{-1} \text{ cm}^{-1}$).

two oxidation levels above **1-BF₄** and that its initial yield was at least 90%. The two-electron reduction of **3-Sc** in the presence of Fc and also its decay to Cu^{I} at elevated temperatures (above -90 °C) are in contrast to the spontaneous one-electron reduction of transient **3** to **2** in the absence of Sc^{3+} ion. This presumably results from much stronger binding of the Sc^{3+} ion to the one-electron-reduced form of **3** due to the increased electron density on the tosylimido group. This would facilitate further reduction to a Cu^{I} complex, accompanied by removal of the imido group with protons as tosylamide. Consistent with this explanation, an independently generated solution of **2** in CH_2Cl_2 was found to be inefficient in oxidizing Fc at -90 °C in the absence of Sc^{3+} ; in the presence of Sc^{3+} , however, **2** was reduced to a Cu^{I} species with the corresponding formation of Fc^+ in 90% yield (Figure 2 inset). A similar effect of Sc^{3+} ion was demonstrated previously by Fukuzumi et al.¹⁶ in the reduction of the complex cation $[\text{Fe}^{\text{IV}}(\text{O})(\text{TMC})]^{2+}$ (TMC = 1,4,8,11-tetramethyl-1,4,8,11-tetraazacyclotetradecane) in the presence of Fc.

The resonance Raman (rR) spectrum of **3-Sc** using 514 nm laser excitation in resonance with the 530 nm transition (inset in Figure 1 top) displays three bands at 570, 660, and 887 cm^{-1} that can be attributed to the $\text{Cu}^{\text{III}}\text{-NTs}/\text{Cu}^{\text{II}}\text{-N}^{\bullet}\text{T}$ s core on the basis of ^{15}N isotope labeling. The band at 887 cm^{-1} showed the largest

$^{15}\text{N}/^{14}\text{N}$ downshift of 24 cm^{-1} , whereas the bands at 570 and 660 cm^{-1} showed a much weaker sensitivity to ^{15}N labeling with downshifts of 2 and 4 cm^{-1} , respectively. The rR spectra thus established the 530 nm band in **3-Sc** as having predominantly nitrene-to-Cu charge transfer character on the basis of the selective enhancement of modes involving Cu–NTs coordinates.

We then turned to X-ray absorption spectroscopy (XAS) to probe the Cu oxidation state in **3-Sc** directly. As expected, complexes **1-BF₄** and **2** exhibited X-ray absorption near-edge structure (XANES) features characteristic of Cu^{I} and Cu^{II} , respectively (Figure 1 bottom).¹⁷ The edge features for **3-Sc** were altered relative to **2**, with a hypsochromic shift of ca. 1 eV in the energies of the two inflection points along the rising edge (Figure S4). However, while the intensity of the pre-edge feature weakened significantly in **3-Sc**, its position at ca. 8978 eV was unchanged from that of **2** (Figure S5). Edge energies are known to be an ambiguous predictor for identifying whether a given complex is Cu^{II} or Cu^{III} , reflecting the fact that the Cu edge includes $1s$ -to- $4p$ transitions that are strongly influenced by donor ligands and geometric structure. Instead, the energy of the pre-edge feature associated with a $1s$ -to- $3d$ transition provides the most reliable basis for identifying Cu^{III} complexes, as this feature typically is upshifted by 2 eV relative to those of Cu^{II} congeners.^{13,18} The absence of a hypsochromic shift in the pre-edge energy strongly suggests that **3-Sc** contains a Cu^{II} center bound to a nitrene radical, consistent with a $\text{Cu}^{\text{II}}\text{--N}^{\bullet}\text{T}$ s formulation. The present study therefore adds to the very few extant reports where direct evidence of metal-bound nitrene radicals has been obtained.^{5a,b,19}

Unfortunately, the strongly absorbing CH_2Cl_2 solvent prevented us from obtaining data of sufficient quality for an extended X-ray absorption fine structure (EXAFS) analysis of **3-Sc**. Therefore, density functional theory (DFT) calculations were performed to gain insights into the molecular structure of **3-Sc**. All of the calculations were done at the BP86/TZVP level in acetone ($\epsilon = 21$), which successfully reproduced the experimentally observed geometry and, in particular, the trends in the variation of the metal–nitrogen distances in **2** (Tables S2 and S3). The overestimation of the metal–nitrogen distances in the calculated structure by $0.05\text{--}0.08\text{ \AA}$ is typical of DFT functionals. The optimized structure of **3-Sc** in the experimentally observed singlet state (Scheme 1 and Table S4) reveals a bent copper–nitrene unit with a $\kappa^2\text{-N,O}$ binding mode of the NSO_2R tosyl nitrene ligand, consistent with the results of a previous calculation.^{6a} The Cu–N(Sc)Ts distance in **3-Sc** was calculated to be 0.045 \AA shorter than the Cu–NHTs distance in **2** (Table S2). Three Raman-active bands involving the Cu–N(Sc)Ts core were calculated, and their positions and $^{15}\text{N}/^{14}\text{N}$ isotopic shifts were in reasonable agreement with the experimental values, thereby validating the proposed structure of **3-Sc** (Figure S6; also see the animation of the vibrational motions provided in the SI). On the basis of the calculations, the experimentally observed rR band at 887 cm^{-1} ($^{15}\text{N}/^{14}\text{N}$ shift of 24 cm^{-1}) is assigned to a symmetric bending of the N–Cu–S angle (Figure S6a); the calculated frequency was 882 cm^{-1} with a shift of 16 cm^{-1} . The remaining ^{15}N -sensitive rR bands at 660 cm^{-1} ($^{15}\text{N}/^{14}\text{N}$ shift of 4 cm^{-1}) and 570 cm^{-1} ($^{15}\text{N}/^{14}\text{N}$ shift of 2 cm^{-1}), on the other hand, correspond to Cu–N stretching modes that are strongly coupled to the vibrations of the tosyl and scandium moieties; the calculated frequencies were 654 cm^{-1} with an $^{15}\text{N}/^{14}\text{N}$ shift of 3 cm^{-1} (Figure S6b) and 589 cm^{-1} with an $^{15}\text{N}/^{14}\text{N}$ shift of 1 cm^{-1} (Figure S6c), respectively. The slight

underestimation of the calculated $^{15}\text{N}/^{14}\text{N}$ shifts by $1\text{--}8\text{ cm}^{-1}$ implies that DFT predicts a slightly different mode composition.

The oxidative reactivity of **3-Sc** was examined for the oxidation of hydrocarbons with C–H bond dissociation energies²⁰ (BDEs) of $67.9\text{--}99.5\text{ kcal mol}^{-1}$. Product analysis of the reaction solutions revealed the formation of the amination or dehydrogenation products in yields of $85\text{--}35\%$ (Scheme 1 and Table S5); the yields decreased with increasing C–H bond strength. The kinetics of the reaction could be followed by UV-vis spectroscopy (Figures S7–S9) at $-90\text{ }^\circ\text{C}$ when 1-benzyl-1,4-dihydronicotinamide (BNAH), xanthene, dihydroanthracene (DHA), 1,4-cyclohexadiene (CHD), triphenylmethane, fluorene, and toluene were used as substrates.

The rates of the reactions were found to be linearly correlated with the BDEs of the substrates (Figure 3), thereby revealing a

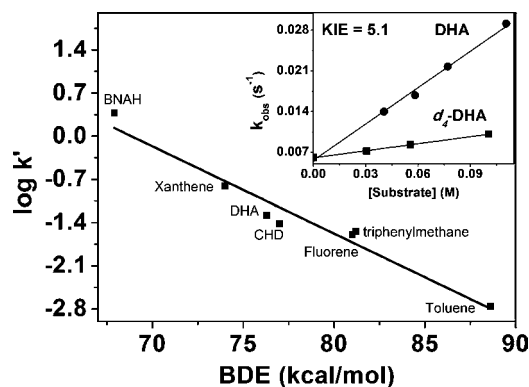


Figure 3. Plot of $\log k'$ for reactions with **3-Sc** at $-90\text{ }^\circ\text{C}$ against the BDEs for different C–H substrates. k' was determined by dividing the second-order rate constant (k_2) by the number of equivalent H atoms in the substrate. Inset: Plot of pseudo-first-order rate constants (k_{obs}) against different concentrations of DHA and d_4 -DHA. The point at zero substrate concentration corresponds to the pseudo-first-order rate constant for the self-decay of **3-Sc** at $-90\text{ }^\circ\text{C}$.

rate-determining H-atom abstraction process. Furthermore, a deuterium kinetic isotope effect (KIE) of 5.1 was obtained when d_4 -DHA was used as a substrate at $-90\text{ }^\circ\text{C}$ (Figure 3 inset). The reaction of **3-Sc** with cyclohexane was found to be too slow relative to its self-decay at $-90\text{ }^\circ\text{C}$; thus, the kinetics could not be monitored. However, when a solution of **3-Sc** was allowed to warm to $25\text{ }^\circ\text{C}$ in the presence of 20 equiv of cyclohexane, a 35% yield of the aminated products was obtained. Additionally, **3-Sc** could also initiate aziridination of cyclohexene and nitrene transfer to triphenylphosphine (Figure S10) at $-90\text{ }^\circ\text{C}$ with the respective formation of cyclohexene-*N*-tosylaziridine (60% yield) and *N*-(*p*-toluenesulfonyl)iminotriphenylphosphorane (85% yield).

The reactivity of **2** was also investigated and compared with that of **3-Sc**. In contrast to the strong oxidizing capabilities of **3-Sc**, complex **2** was found to be a sluggish oxidant that reacted only with strong reductants such as triphenylphosphine at $25\text{ }^\circ\text{C}$ to form *N*-(*p*-toluenesulfonyl)iminotriphenylphosphorane (75% yield; Table S5); the reaction was orders of magnitude slower than that with **3-Sc** (Figure S11). Additionally, **2** did not react even at $25\text{ }^\circ\text{C}$ with the weak C–H bonds of DHA or CHD in the presence or absence of scandium.

In summary, we have demonstrated the Lewis acid trapping of an elusive copper–tosyl nitrene complex, **3-Sc**, and shown it to be diamagnetic and two oxidation levels above the Cu^{I} complex **1-BF₄**. The stabilization of **3-Sc** can be attributed to the binding of

Sc³⁺ to the [CuNTs]⁺ core, which may help reduce the strong electron repulsion between the electron-rich nitrene and copper centers, presumably by lowering the electron density at the nitrene nitrogen. In other words, the binding of Sc³⁺ may help to lessen the H-atom abstraction ability of **3**, thereby preventing its spontaneous decay to the copper(II)–amide species **2** (Scheme 1). Consistent with the above explanation, the use of weaker Lewis acids such as Y³⁺, Zn²⁺, and Ca²⁺ instead of Sc³⁺ resulted in a significantly lower yield of the copper–nitrene intermediate and increased formation of **2**.¹² Sufficient stability of **3-Sc** at –90 °C enabled its characterization using a variety of spectroscopic methods, which helped to establish its electronic structure as Cu^{II}–N[•](Sc)Ts with a copper-bound nitrene radical. Additionally, the vibrational modes of the Cu^{II}–N[•](Sc)Ts core have been established through rR and DFT studies, which should help in their elucidation under catalytic turnover conditions. Finally, the present report of the stabilization of the Cu^{II}–N[•]Ts core may validate the existence of the elusive isoelectronic Cu^{III}–O/Cu^{II}–O[•] units, which have been proposed as reactive intermediates in a number of chemical and biological oxidation reactions.²¹ In particular, the ability of **3-Sc** to attack the strong C–H bonds of cyclohexane is extraordinary in the context of the known oxidizing capabilities of copper–dioxygen species.²² With the assumption that the reactivity of the Cu^{II}–N[•]Ts core can be extended to the Cu^{III}–O/Cu^{II}–O[•] core, the present study therefore suggests the possible involvement of Cu^{III}–O/Cu^{II}–O[•] active species in the catalytic cycle of mononuclear copper monooxygenases.

■ ASSOCIATED CONTENT

● Supporting Information

Additional syntheses and characterization data (UV–vis, EPR, NMR), kinetic data, experimental X-ray diffraction parameters and crystal data, computational data, and a figure and an animation showing the vibrational modes arising from the Cu–NTs core. This material is available free of charge via the Internet at <http://pubs.acs.org>.

■ AUTHOR INFORMATION

Corresponding Author

kallol.ray@chemie.hu-berlin.de

Notes

The authors declare no competing financial interest.

■ ACKNOWLEDGMENTS

We gratefully acknowledge financial support of this work from the Cluster of Excellence “Unifying Concepts in Catalysis” (EXC 314/1), Berlin. XAS data were obtained on Beamline X3B of the National Synchrotron Light Source (NSLS, Brookhaven National Laboratory, Upton, NY). Beamline X3B is operated by the Case Western Reserve University Center for Synchrotron Biosciences, supported by NIH Grant P30-EB-009998. NSLS is supported by the U.S. Department of Energy, Office of Science, Office of Basic Energy Sciences, under Contract DE-AC02-98CH10886. We also thank Dr. E. Bill, Prof. F. Neese, and Prof. R. Stößer for access to the EPR instruments and Prof. C. Limberg for access to the GC–MS instrument.

■ REFERENCES

- (1) Kwart, H.; Kahn, A. A. *J. Am. Chem. Soc.* **1967**, *89*, 1950.
- (2) Müller, P.; Fruit, C. *Chem. Rev.* **2003**, *103*, 2905.
- (3) (a) Diaz-Requejo, M. M.; Belderrain, T. R.; Nicasio, M. C.; Trofimenko, S.; Perez, P. J. *J. Am. Chem. Soc.* **2003**, *125*, 12078.

(b) Fructos, M. R.; Trofimenko, S.; Diaz-Requejo, M. M.; Perez, P. J. *J. Am. Chem. Soc.* **2006**, *128*, 11784.

(4) (a) Badiel, Y. M.; Dinescu, A.; Dai, X.; Palomino, R. M.; Heinemann, F. W.; Cundari, T. R.; Warren, T. H. *Angew. Chem., Int. Ed.* **2008**, *47*, 9961. (b) Li, Z.; Quan, R. W.; Jacobsen, E. N. *J. Am. Chem. Soc.* **1995**, *117*, 5889. (c) Diaz-Requejo, M. M.; Perez, P. J.; Brookhart, M.; Templeton, J. L. *Organometallics* **1997**, *16*, 4399.

(5) (a) King, E. R.; Hennesy, E. T.; Betley, T. A. *J. Am. Chem. Soc.* **2011**, *133*, 4917. (b) Lyaskovskyy, V.; Suarez, A. I. O.; Lu, H.; Jiang, H.; Zhang, X. P.; de Bruin, B. J. *Am. Chem. Soc.* **2011**, *133*, 12264. (c) Waterman, R.; Hillhouse, G. L. *J. Am. Chem. Soc.* **2008**, *130*, 12628.

(6) (a) Brandt, P.; Södergren, M. J.; Andersson, P. G.; Norrby, P.-O. *J. Am. Chem. Soc.* **2000**, *122*, 8013. (b) Gillespie, K. M.; Crust, E. J.; Deeth, R. J.; Scott, P. *Chem. Commun.* **2001**, 785. (c) Tekarli, S. M.; Williams, T. G.; Cundari, T. R. *J. Chem. Theory Comput.* **2009**, *5*, 2959. (d) Cundari, T. R.; Dinescu, A.; Kazi, A. B. *Inorg. Chem.* **2008**, *47*, 10067.

(7) Liang, H.-C.; Zhang, C. X.; Henson, M. J.; Sommer, R. D.; Hatwell, K. R.; Kaderli, S.; Zuberbühler, A. D.; Rheingold, A. L.; Solomon, E. I.; Karlin, K. D. *J. Am. Chem. Soc.* **2002**, *124*, 4170.

(8) Macikenas, D.; Skrzypczak-Jankun, E.; Protasiewicz, J. D. *J. Am. Chem. Soc.* **1999**, *121*, 7164.

(9) (a) Gonzalez-Alvarez, M.; Alzuet, G.; Borrás, J.; Agudo, L. C.; Garcia-Granda, S.; Bernardo, J. M. M. *J. Inorg. Biochem.* **2004**, *98*, 189. (b) Macias, B.; Villa, M. V.; Gomez, B.; Borrás, J.; Alzuet, G.; Gonzalez-Alvarez, M.; Castineiras, A. *J. Inorg. Biochem.* **2007**, *101*, 444.

(10) Que, L. Jr. *Physical Methods in Bioinorganic Chemistry: Spectroscopy and Magnetism*; University Science Books: Sausalito, CA, 2000.

(11) Pfaff, F. F.; Kundu, S.; Risch, M.; Pandian, S.; Heims, F.; Pryjomska-Ray, I.; Haack, P.; Metzinger, R.; Bill, E.; Dau, H.; Comba, P.; Ray, K. *Angew. Chem., Int. Ed.* **2011**, *50*, 1711.

(12) Other metal ions could also be used to generate the formal Cu^{III} purple intermediate; however, the yields (Figure S12 and Table S6) decreased in the order Sc³⁺ (90%) > Y³⁺ (54%) > Zn²⁺ (28%) > Ca²⁺ (0%), which follows the order of decreasing Lewis acidity of the metal ions. See: Fukuzumi, S.; Ohkubo, K. *J. Am. Chem. Soc.* **2002**, *124*, 10270.

(13) Donoghue, P. J.; Tehranchi, J.; Cramer, C. J.; Sarangi, R.; Solomon, E. I.; Tolman, W. B. *J. Am. Chem. Soc.* **2011**, *133*, 17602.

(14) King, A. E.; Huffman, L. M.; Casitas, A.; Costas, M.; Ribas, X.; Stahl, S. S. *J. Am. Chem. Soc.* **2010**, *132*, 12068.

(15) The formation of Cu^I was inferred from EPR studies (it was EPR-silent) and UV–vis studies (no Cu^{II} d–d bands were observed).

(16) Fukuzumi, S.; Morimoto, Y.; Kotani, H.; Naumov, P.; Lee, Y.-M.; Nam, W. *Nat. Chem.* **2010**, *2*, 756.

(17) Kau, L. S.; Spira-Solomon, D. J.; Penner-Hahn, J. E.; Hodgson, K. O.; Solomon, E. I. *J. Am. Chem. Soc.* **1987**, *109*, 6433.

(18) DuBois, J. L.; Mukherjee, P.; Stack, T. D. P.; Hedman, B.; Solomon, E. I.; Hodgson, K. O. *J. Am. Chem. Soc.* **2000**, *122*, 5775.

(19) Lu, C. C.; George, S. D.; Weyhermüller, T.; Bill, E.; Bothe, E.; Wieghardt, K. *Angew. Chem., Int. Ed.* **2008**, *47*, 6384.

(20) Luo, Y.-R. *Comprehensive Handbook of Chemical Bond Energies*; CRC Press: Boca Raton, FL, 2007.

(21) (a) Yoshizawa, K.; Kihara, N.; Kamachi, T.; Shiota, Y. *Inorg. Chem.* **2006**, *45*, 3034. (b) Crespo, A.; Marti, M. A.; Roitberg, A. E.; Amzel, L. M.; Estrin, D. A. *J. Am. Chem. Soc.* **2006**, *128*, 12817. (c) Hong, S.; Huber, S. M.; Gagliardi, L.; Cramer, C. C.; Tolman, W. B. *J. Am. Chem. Soc.* **2007**, *129*, 14190.

(22) (a) Lewis, E. A.; Tolman, W. B. *Chem. Rev.* **2004**, *104*, 1047. (b) Himes, R. A.; Karlin, K. D. *Curr. Opin. Chem. Biol.* **2009**, *13*, 119.